Generalized Reynolds number and viscosity definitions for non-Newtonian fluid flow in ducts of non-uniform cross-section

D. Crespí-Llorens[b], P. Vicente[b], A. Viedma[a]

[a]*Dep. Ing. Térmica y de Fluidos. Universidad Politécnica de Cartagena. Dr. Fleming, s/n (30202). Cartagena (Spain).*
[b]*Dep. Ing. Mecánica y Energía. Universidad Miguel Hernández. Av. Universidad, s/n (03202). Elche (Spain). dcrespi@umh.es*

Abstract

This work presents and experimental study of the generalization method of the Reynolds number and the viscosity of pseudoplastic fluid flow in ducts of non-uniform cross-section. This method will permit to reduce 1 degree of freedom of hydrodynamical and thermal problems in those ducts. A review of the state of the art has been undertaken and the generalization equation proposed for ducts of uniform cross section has been used as a starting point. The results obtained with this equation have not been found satisfactory and a new one has been proposed.

Specifically, the procedure has been developed for two models of scraped surface heat exchanger with reciprocating scrapers. For both models, the scraper consists of a concentric rod inserted in each tube of the heat exchanger, mounting an array of plugs that fit the inner tube wall. The two models studied differ in the design of the plug.

The procedure to perform the generalization method out of experimental data is accurately detailed in the present document.

Keywords: non Newtonian, viscosity, generalized Reynolds number, non-uniform cross-section, Power Law

Nomenclature

m	flow consistency index (rheological property),	[Pa.s^n]
D	inner diameter of the heat exchanger pipe,	[m]
D_v	inner diameter of the viscometer pipe,	[m]
d	diameter of the insert device shaft,	[m]
D_h	hydraulic diameter $D_h = D - d$,	[m]
L_p	pipe length between pressure ports of test section,	[m]
L_v	viscometer pipe length between pressure ports,	[m]
N	number of measures for each experiment	
P	pitch of the insert devices,	[m]
p	pressure,	[Pa]
p_L	pressure drop by length unit,	[Pa/m]
Q	flow rate,	[m^3/s]
S	main cross-section,	[m^2]
u_b	bulk velocity,	[m/s]

Dimensionless numbers

n	flow behaviour index (rheological property)
Re	Reynolds number, $Re = \rho u_b D_h / \mu$

f	Fanning friction factor, $f = \Delta p D_h / 2L\rho u_b^2$	
ξ	pressure drop constant dependent on the duct geometry	
a to e	correlation constants	

Greek Symbols

α	exponent of Re_b in experimental correlations,	$[s^{-1}]$
γ	shear rate,	$[s^{-1}]$
μ	fluid viscosity (exact definition indicated by the subindex),	[Pa.s]
ϕ	function of n	
Ψ	unknown function,	$[kg/m^3]$
ρ	fluid density,	$[kg/m^3]$
τ	shear stress,	[Pa]

Subscripts

b	Reynolds number or viscosity defined by Eq. 2
g	Reynolds number or viscosity defined by Eqs. 18 and 19
MR	defined by Metzner and Reed (1955) (Eqs. 4and 5)
DL	defined using the equation from Delplace and Leuliet (1995) (Eqs. 6 and 7)
$\xi = an$	generalization based on pressure drop in annulus, where ξ is obtained from Kozicki et al. (1966))

$\xi = exp$ ξ in Eqs. 6 and 7 is obtained by experimental correlation

v belonging to the viscometer

w at the inside pipe wall

1. Introduction

Many fluids in the food and chemical or petrochemical industries are non-Newtonian. In such applications the determination of parameters such as the friction factor and the Nusselt number is necessary for the calculation of pressure losses and heat transfer rates or temperature distributions in heat exchangers. This can be achieved experimentally or theoretically by solving the appropriate transport equations for typical common geometries (circular ducts, flat ducts, etc.). An important characteristic of these fluids is that they have large apparent viscosities; therefore, laminar flow conditions occur more often than with Newtonian fluids.

Pseudoplastic fluids are the most common non-Newtonian fluids in the process industry Chhabra and Richardson (2008); Cancela et al. (2005). For this fluids, in a certain range of shear stress, the viscosity decreases as shear stress increases. To describe this behaviour, various mathematical models can be used. Among them, the Power Law model is widely used because of its simplicity. The model can be used to explain the viscosity of a specific fluid in a limited range of shear rates. The Power Law model (Eq. 1) has two parameters: the flow behaviour index n and the flow consistency index m. Thus, the hydrodynamic and thermal problems have one additional degree

of freedom, which increases their complexity.

$$\tau = m\gamma^n \tag{1}$$

For example, let us consider the study of pressure drop in fully developed flow in pipes for forced convection. The list of significant variables can be $p_L = \Psi(D, u_b, \rho, m, n)$. Through the Pi Theorem the problem simplifies to three non-dimensional numbers $f = \Psi(Re, n)$. Consequently, the relation between Re and the friction factor will be different for fluids with different n. With the previous list of variables, the Reynolds number for power law fluids would be,

$$Re_b = \frac{\rho u_b^{2-n} D^n}{m} = \frac{\rho u_b D}{\mu_b} \tag{2}$$

, where viscosity would be defined by $\mu_b = m(u_b/D)^{n-1}$. Other viscosity definitions, with the same dimensional equations, are possible and will be more useful for the study of pressure drop in heat exchangers.

Metzner and Reed (1955) where the first to use the so called generalization method. They analytically obtained the relation between the friction factor f and the Reynolds number Re_b for the fully developed laminar flow in a pipe. Then, they defined a new Reynolds number Re_{MR}, being the one which multiplied by the friction factor gave the same result that the one given by a Newtonian fluid.

$$f \times Re_{MR} = 16 \tag{3}$$

$$Re_{MR} = \frac{\rho u_b^{2-n} D^n}{m\ 8^{n-1}\left((3n+1)/(4n)\right)^n} = \frac{\rho u_b D}{\mu_{MR}} \tag{4}$$

, being the generalized viscosity for the flow in pipes

$$\mu_{MR} = m\left(\frac{u_b}{D_h}\right)^{n-1} 8^{n-1}\left(\frac{3n+1}{4n}\right)^n \tag{5}$$

Kozicki et al. (1966) obtained a relation between friction factor and Reynolds number for various simple geometries (circular pipes, parallel plates, concentric annuli and rectangular, isosceles triangular and elliptical ducts) as a function of two parameters. Afterwards, Delplace and Leuliet (1995) reduced those parameters to one. Therefore, the definition of Metzner and Reed (1955) can be applied to geometries with uniform cross-section as a function of a single geometric constant.

$$Re_{DL} = \frac{\rho u_b^{2-n} D_h^n}{m \times \xi^{n-1} \left(\frac{24n+\xi}{(24+\xi)n}\right)^n} \tag{6}$$

$$\mu_{DL} = m \left(\frac{u_b}{D_h}\right)^{n-1} \xi^{n-1} \left(\frac{24n+\xi}{(24+\xi)n}\right)^n \tag{7}$$

$$f \times Re_{DL} = 2\xi \tag{8}$$

For duct geometries of uniform cross-section different from the ones studied by Kozicki et al. (1966), similar relations can be obtained either experimentally or numerically. This simplification leads to significant reduction in the study cases of a particular problem. This has been called a generalization method because it allows to express the pressure drop behaviour of Newtonian and non-Newtonian fluids with a single curve. Consequently, the Reynolds number and viscosity defined by this method are known as the *generalized Reynolds number* and the *generalized viscosity* (Kakaç et al., 1987; Chhabra and Richardson, 2008). Besides, the generalized viscosity can be used to generalize other dimensionless numbers such as the Prandtl number in non isothermal flows (Hartnett and Kostic, 1985; Delplace and Leuliet, 1995).

The described method has been used by many authors until recent days (Gratao et al., 2006, 2007; Giri and Majumder, 2014). But, as mentioned

before, it can only be applied to ducts with uniform cross-section, where the shear-stress at the wall is uniform along the duct.

Enhanced heat exchangers EHE (Hong and Bergles, 1976; Marner and Bergles, 1985) are widely used in the process industry in order to enhance heat transfer and they work often with non-Newtonian fluids. Webb (2005) classified enhancement techniques into active, if they require external power, and passive, if they do not. Active techniques as scraped surface heat exchangers SSHE are specially designed to avoid fouling and enhance heat transfer. This last kind of enhanced heat exchanger is specially useful for the work with non-Newtonian fluids because of their high viscosity (Nazmeev, 1979). In most EHE designs, specially in SSHE, the cross-section varies along their length or else the cross-section is uniform but complex and has not previously been studied. Therefore, the generalization method must be based on experimental or numerical results and it is not straightforward.

To overcome this inconvenience, most authors have considered their geometry to be very similar to one of the simple uniform cross-section geometries studied by Kozicki et al. (1966) or Metzner and Reed (1955). This is the case of corrugated pipes or pipes with wire coil or twisted tape inserts. Manglik et al. (1988); Oliver and Shoji (1992); Patil (2000); Martínez et al. (2014) took this option for their studies of passive EHE performance with non-Newtonian fluids and Igumentsev and Nazmeev (1978) did so for his study of SSHE. However, there are complex geometries where this assumption is not valid at all. For those cases, Delplace and Leuliet (1995) proposed the use of experimental methods to obtain the value of ξ. Based on the previous research of Rene et al. (1991), they proposed to use $\xi = 56.6$ for a plate heat

exchanger type. Afterwards some other researchers have broaden Rene et al. (1991) and Delplace and Leuliet (1995) studies with numerical simulations in the same plate heat exchangers model (Fernandes et al., 2007, 2008) varying some design parameters.

Our extensive literature search has not yielded further researches about the generalization method of viscosity in complex geometries with non-uniform cross section. In view of this situation the present study was undertaken.

The present paper presents a simplified generalization method for the Reynolds number and fluid viscosity, based on the studies of Metzner and Reed (1955) and Delplace and Leuliet (1995), which can be applied to ducts of non-uniform cross-section. In order to prove its validity, pressure drop has been measured experimentally in two different pipe axial reciprocating scraped surface heat exchangers AR-SSHE. These geometries are shown in Fig. 1.

2. Experimental Set-up

The experimental setup shown in Fig. 2 has been used to measure pressure drop for different flow regimes in axial reciprocating scraped surface heat exchangers (Fig. 1(a) and Fig. 1(b)). The experimental facility consists of two independent circuits. The primary circuit, which contains the test fluid, is divided in two sub-loops. The test section is placed in the main one, including a gear pump (2) driven by a frequency controller (3). The test fluid in the supply tank (1) is continuously cooled in the second sub-loop through a plate heat exchanger (13) with a coolant flow rate settled by a three-way valve (15). The coolant liquid of the secondary circuit is stored in

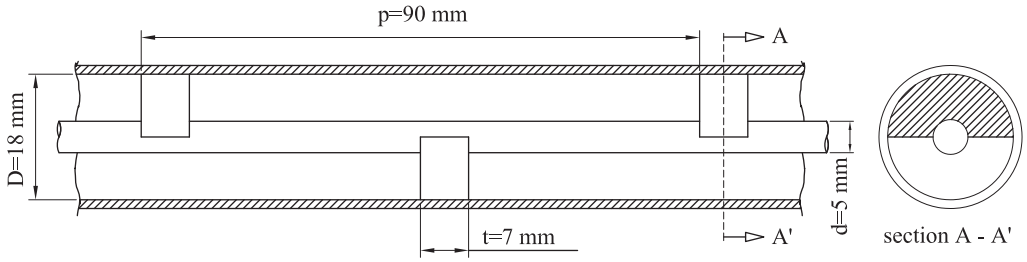

(a) EG1 geometry of an scraped surface heat exchanger.

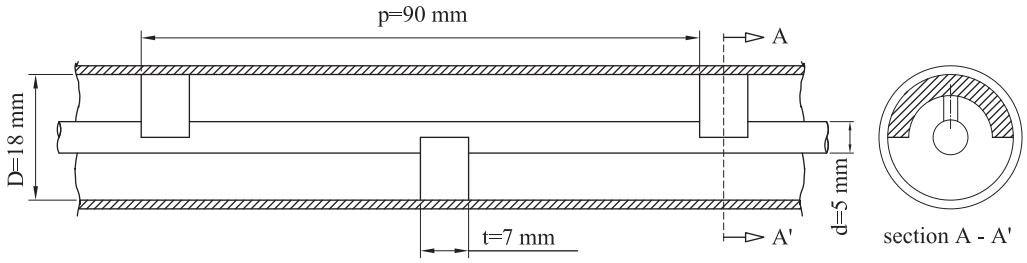

(b) EG2 geometry of an scraped surface heat exchanger.

Figure 1: Analysed geometries.

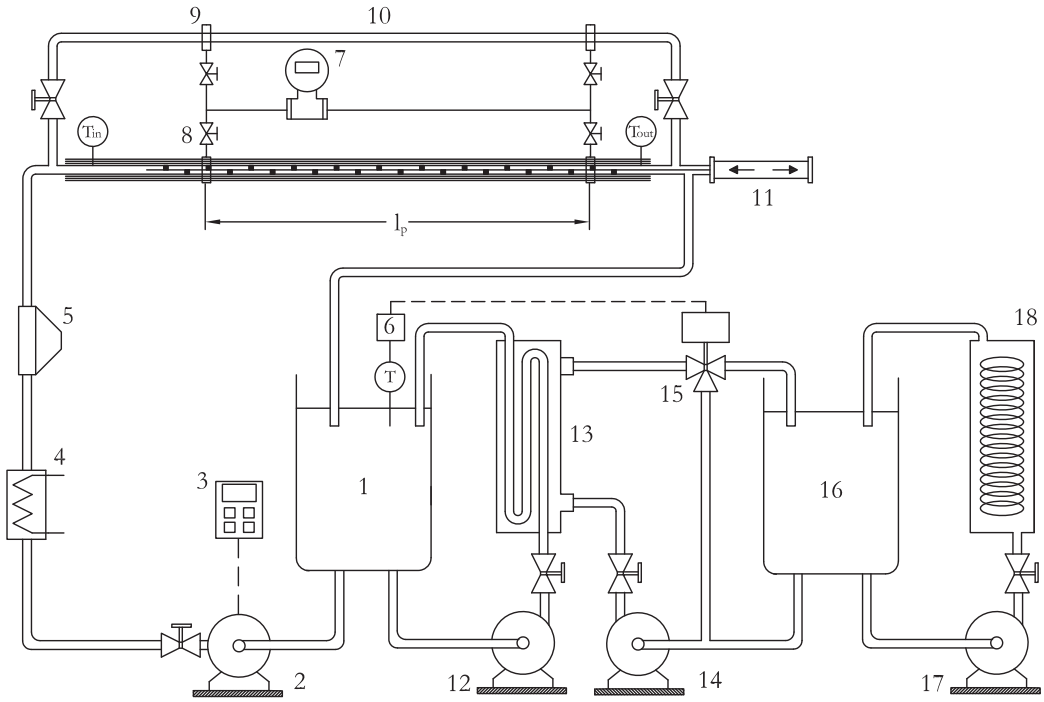

Figure 2: Experimental set-up. (1) Test fluid tank, (2, 12) gear pumps, (3) frequency converter, (4) immersion resistance, (5) Coriolis flowmeter, (6) RTD temperature sensor, (7) pressure transmitter, (8) stainless steel tube with an insert scraper and with inlet and outlet immersion RTDs, (9) pressure ports, (10) smooth stainless steel pipe used as viscometer, (11) hydraulic piston (14, 17) centrifugal pumps, (15) three-way valve with a PID controller, (16) coolant liquid tank, (18) cooling machine.

a 1000 l tank (16) from where it flows to a cooling machine. The thermal inertia of this tank, with a capacity of 1000 l, together with the operation of the PID-controlled three way valve provides stability to the temperature of the test fluid in the supply tank, which can be accurately fixed to a desired value. The test section was placed in the main circuit and consisted of a thin-walled, 4 m long, 316L stainless steel tube with an insert scraper. The inner and outer diameters of the tube were 18 mm and 20 mm, respectively. Two oversize, low-velocity gear pumps (one on each circuit) were used for circulating the working fluid, in order to minimize fluid degradation during the tests. Mass flow rate and fluid density was measured by a Coriolis flow meter, which performs properly when working with non-Newtonian fluids (Fyrippi et al., 2004). Four pressure taps separated by 90° were coupled to each end of the pressure test section of 1.85 m length. A long test section has been used to improve measurement precision. Pressure drop Δp_{E1} and Δp_{E2} was measured by means of two highly accurate pressure transmitters LD-301 configured for different ranges. Pressure measurement ports were separated a distance $L_p = 20 \times P$, and consisted of four pressure holes peripherally spaced by 90°. Test section was preceded by a development region of $L_e = 6 \times P$ length, in order to establish periodic flow conditions.

The rheological properties of the non-Newtonian test fluid n and m is measured by an in-line viscometer, parallel to the testing tube. In that way, measurements of the rheological properties could be done at the beginning and at the end of each set of experiments, minimizing the thixotropy effect. Further details are given in next section.

Further details of the working apparatus and the calibration procedure

are given in Solano et al. (2011) and García et al. (2005).

2.1. Test fluid characteristics

The test fluid was 1% wt aqueous solutions of carboxymethyl cellulose (CMC), supplied by SigmaAldrich Co. CMC with different chain length have been used: medium viscosity (ref. C4888, 250 kDa), high viscosity (ref. C5013, 700 kDa) and ultra high viscosity (ref. 21904). The solutions were prepared by dissolving the polymer powder in distilled water and then raising the pH values of the solution to increase viscosity. This fluid shows a non-Newtonian pseudoplastic behaviour well described by the Power Law model of Eq. 1 for a big range of shear rates (Abdelrahim and Ramaswamy, 1995; Ghannam and Esmail, 1996; Abu-Jdayil, 2003; Yang and Zhu, 2007), although it presents a Newtonian plateau for shear rates under 0.1 s^{-1} (Benchabane and Bekkour, 2008).

All CMC thermophysical properties but the rheological parameters and fluid density were assumed to be the same as pure water (Chhabra and Richardson, 2008; Cancela et al., 2005).

Rheological fluid properties are strongly influenced by the type of CMC powder employed, the preparation method and fluid degradation due to shear stress and thermal treatment. The combination of those factors allows to obtain fluids with different pseudoplastic behaviour, ranging from $n = 0.45$ to $n = 1$.

The values of n and m for the test fluid were obtained by using the in-line smooth pipe as a viscometer. In the smooth pipe, flow rate Q and pressure drop Δp are measured 20 times for four different flow rates. Bulk velocity u_b and shear stress at the wall τ_w are obtained out of flow rate and pressure

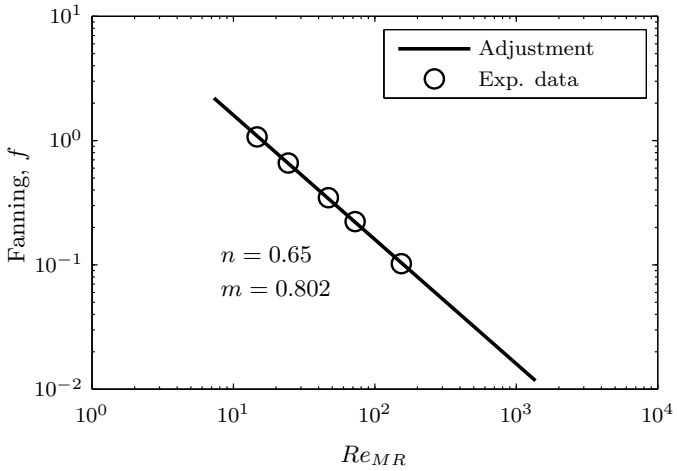

Figure 3: Rheological properties measurement during one of the test.

drop respectively

$$\tau_w = \frac{\Delta p D_v}{4L} \tag{9}$$

, as the velocity profile of the fully developed isothermal flow of power law fluids in pipes is well known, τ_w can also be derived from the constitutive Eq. 1,

$$\tau_w = m \left[\frac{8u_b}{D_v} \left(\frac{3n+1}{4n} \right) \right]^n \tag{10}$$

, whose logarithm yields

$$ln(\tau_w) = n \times ln(u_b) + ln(m) + n \times ln \left[\frac{8u_b}{D_v} \left(\frac{3n+1}{4n} \right) \right] \tag{11}$$

, out of which the rheological properties m and n can be obtained by adjusting the experimental data with a least squared method. An example of a rheological measurement result is shown in Fig. 3.

Because of fluid degradation, rheological properties must be obtained frequently. Experiments are planned in sets of 15 to 25 and rheological properties are obtained before and after each set. A maximum of 3% deviation between rheological properties measurements has been obtained. Degradation between measurements has been supposed to be linear with experimenting time, so that m and n can be obtained for each experiment.

2.2. Accuracy of the experimental data

The experimental uncertainty was calculated by following the "Guide to the expression of uncertainty in measurement", published by the ISO (1995). On one hand, the Coriolis flowmeter has a repeatability of 0.025 % of the flow rate measure, while its precision when measuring density is 0.2 kg/m^3. On the other hand, pressure sensor has a repeatability of 0.075 of its range. Uncertainties of the heat exchanger and viscometer dimensions have been assigned according to the measuring tool employed. The uncertainty associated to rheological properties are obtained out of the least squares adjustment. The maximum uncertainty of n and m are 0.01% and 0.4% respectively.

A summary of the uncertainties of dimensions and sensor measurements is shown in Table 1. The resulting error for Re_b and f are of 1.2% and 2% respectively.

3. Results

Friction factor measurements in EG1 and EG2 geometries are plotted in Fig 4 versus Re_b defined by Eq. 2. As it can be appreciated the friction factor f is a function of Re_b and the flow behaviour index n.

(a) Dimensions.

Variable	Value	Uncertainty	Units	Uncert. (%)
D	18	$0.05/\sqrt{3}$	mm	0.2
d	5	$0.05/\sqrt{3}$	mm	0.6
D_h	13	0.04	mm	0.3
S	234.8	0.7	mm^2	0.4
D_v	16	$0.05/\sqrt{3}$	mm	0.2
S_v	201.1	0.8	mm^2	0.4
L_v	1885	$0.5/\sqrt{3}$	mm	0.02
L_p	1850	$0.5/\sqrt{3}$	mm	0.02

(b) Sensors measurements. N is the number of measurements.

Variable	Value	N	Uncertainty	Units	Max. Uncert. (%)
Δp_{E1}	$10 - 405$	$20 - 10$	$0.07 - 0.09$	mbar	0.7
Δp_{E2}	$400 - 2500$	10	0.6	mbar	0.1
Q	$30 - 2000$	$10 - 20$	-	kg/h	7.9×10^{-3}
ρ	1000	1	0.1	kg/m^3	0.01

Table 1: Uncertainties in dimensions and sensor measurements.

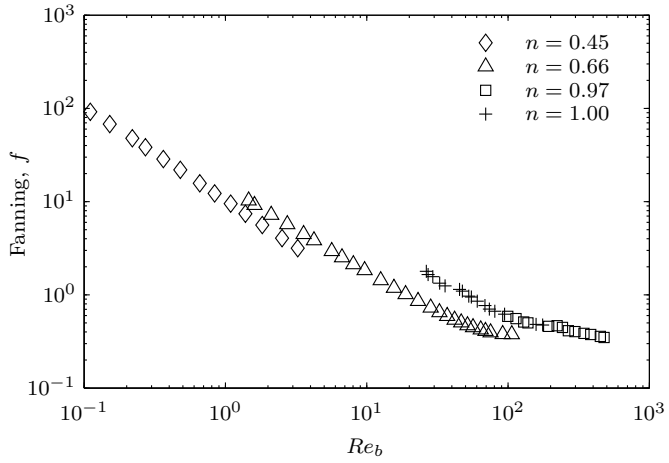

(a) EG1

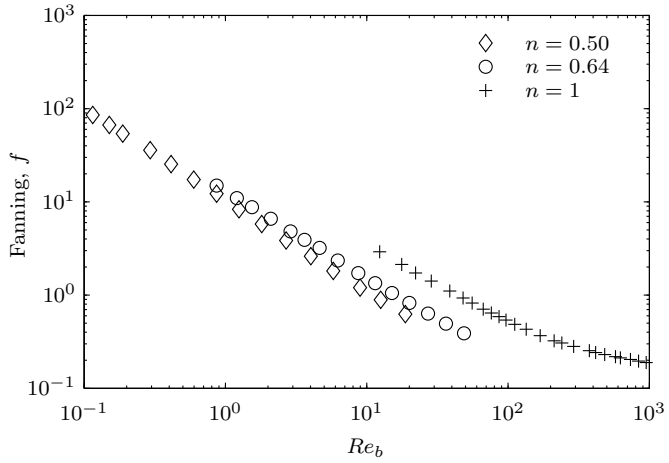

(b) EG2

Figure 4: Re_b versus Fanning friction factor for the geometries under study. Only most representative results are shown.

3.1. Generalization based on annulus geometry

Geometries of EG1 and EG2 scraped surface heat exchangers are similar to an annular passage. Therefore, a generalization method based on the annulus geometry may be a good approach for these cases. For this value of the radius ratio ($d/D = 5/18$), the value of $\xi = 11.69$ can be obtained from Kozicki et al. (1966).

In Fig. 5, $f \times Re_b$ versus n has been plotted for the experiments and for the solution in annulus given by Eq. 6 with $\xi = 11.69$. As it can be observed, annulus results underpredict experimental ones in 34% on average for EG1 and in 27% on average for EG2. Pressure drop results are shown in Fig. 6 and Fig. 7, where the generalized Reynolds number has been defined for the mentioned value of ξ. As it can be observed, the results show different curves for each fluid with different value of n and measurements do differ from the theoretical solution in annulus. Therefore it can be concluded that the generalization method is not valid in these cases.

However, some useful information can be obtained from Figures 6 and 7. For $Re_{DL,\xi=an} < 100$ the flow is laminar and above this range the transitional flow starts. Besides, it can be observed that the distance between experimental results and the line representing the annulus solution varies with $Re_{DL,\xi=an}$, meaning that $f \not\propto Re_b^{-1}$.

3.2. Experimental value of ξ

In this subsection, the solution suggested by Delplace and Leuliet (1995) has been used for the generalization method. They proposed to use Eq. 8, what has been modified to include an exponent for the Reynolds number, α,

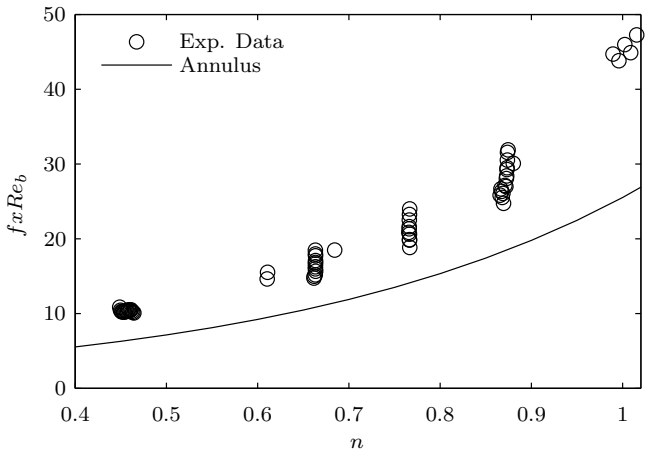

(a) EG1

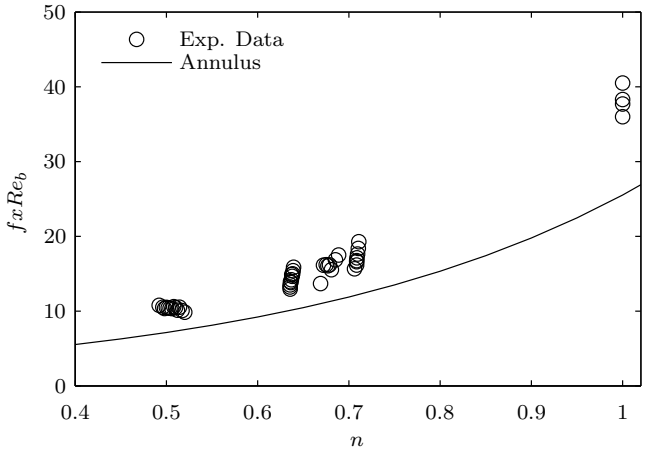

(b) EG2

Figure 5: Comparison of $f \times Re_b$ between experimental results and theoretical results for annulus.

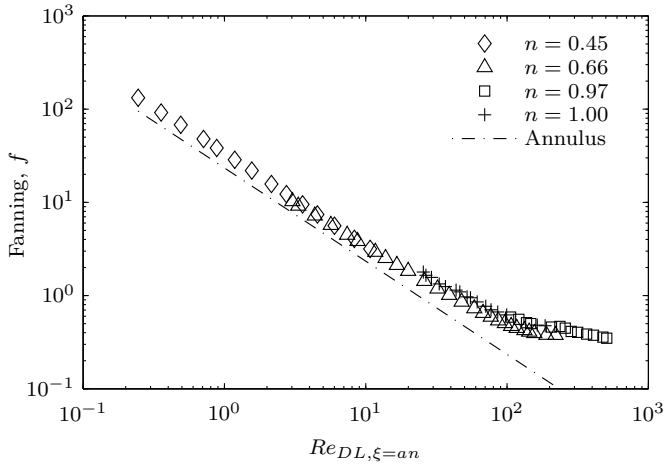

(a) Whole Reynolds range

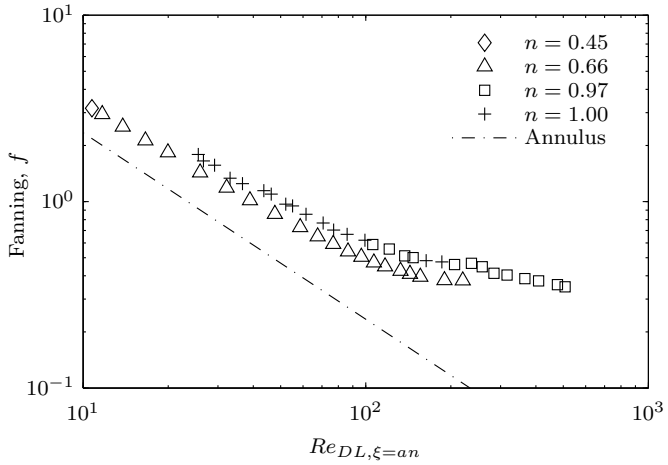

(b) Narrower Reynolds range

Figure 6: EG1. $Re_{DL,\xi=an}$ versus Fanning friction factor.

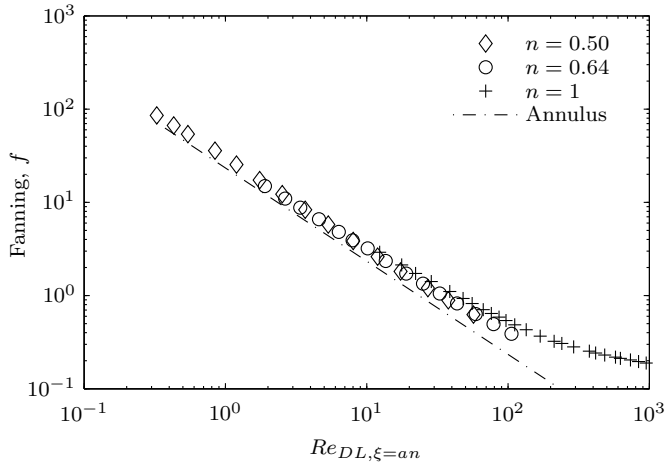

(a) Whole Reynolds range

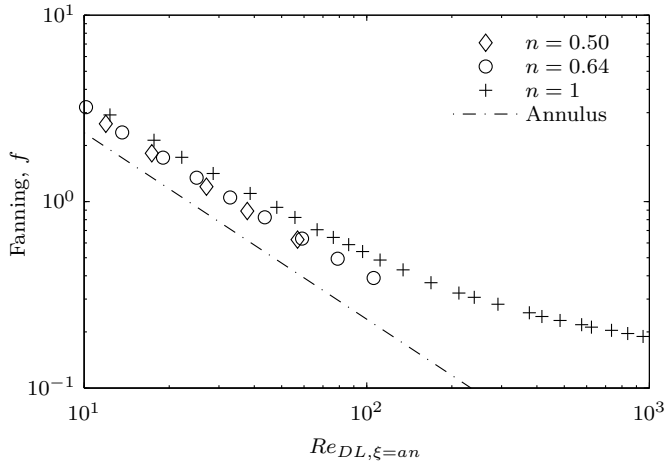

(b) Narrower Reynolds range

Figure 7: EG2. $Re_{DL,\xi=an}$ versus Fanning friction factor.

as it has been explained in previous section,

$$f \times Re_b^{\alpha} = 2\xi^n \left(\frac{24n + \xi}{(24 + \xi)n} \right)^n \tag{12}$$

The experimental data has been correlated to obtain the value of ξ in Eq. 12. For this, only experiments with Reynolds numbers under 40 (highly laminar region) have been considered. The reason for doing this is that, although laminar region ends at Reynolds number about 100, the exponent of the Reynolds number in Eq. 12 decreases with the Reynolds number along the laminar region, what becomes significant for Reynolds numbers above 40. The goal is not to obtain an experimental correlation for the data in the laminar region but to obtain a proper definition of the generalized Reynolds number, valid for the whole laminar region.

The experimental values of ξ for EG1 and EG2, and the corresponding uncertainties for a confidence level of 95 % are shown in Table 2[1]. The experimental data and Eq. 12 with the calculated values of ξ for both geometries are plotted in Fig. 8. Besides, friction factor versus the generalized Reynolds number (with this ξ) is plotted in Fig. 9.

Table 2: Experimental correlation for ξ in Eq. 12 (Delplace and Leuliet, 1995).

	α	ξ	Error
EG1	0.974	19.38	17.0%
EG2	0.951	16.67	13.3%

[1]The procedure to obtain α is explained in section 3.4.

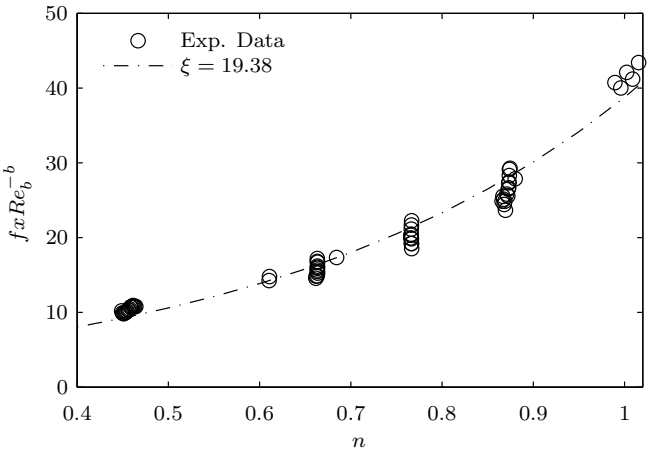

(a) EG1

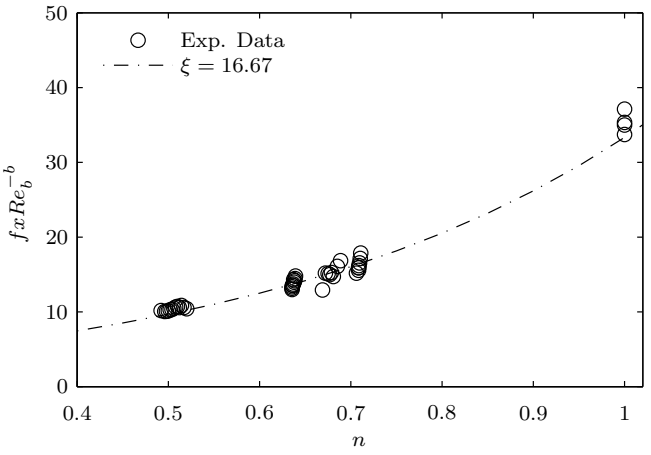

(b) EG2

Figure 8: Comparison between experimental results and Eq. 12 with the experimental values of ξ (see Table 2)

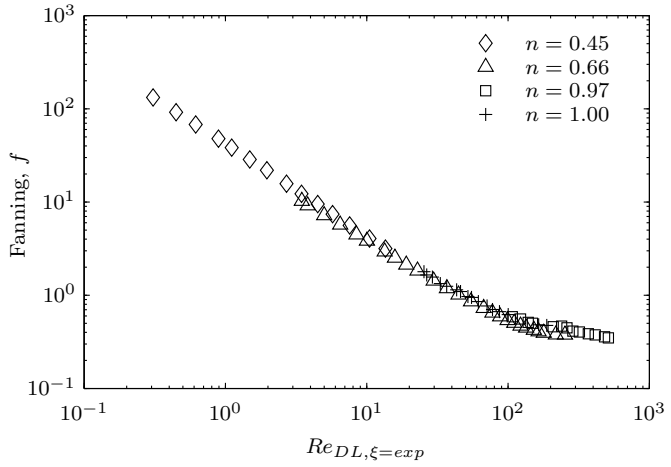

(a) EG1

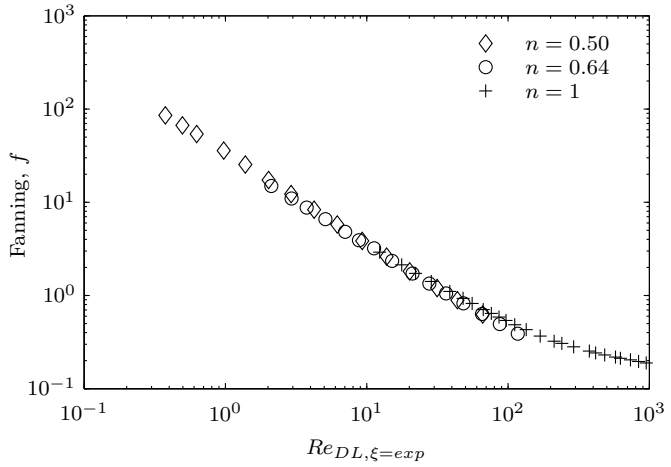

(b) EG2

Figure 9: Generalized Reynolds number with Eq. 12 and the experimental values of ξ (see Table 2).

Results in Fig. 8 show an under prediction of the product $f \times Re_b^{\alpha}$ for $n \approx 0.45$ and $n \approx 1$ for both geometries. Furthermore, it can be observed in Fig. 9 that the experimental results for different n do not collapse to the same curve. This effect is higher in EG1 geometry, where the flow is significantly different from the annulus geometry. Results of this generalization method are still not satisfactory.

3.3. Proposed experimental correlations

At this point, an experimental correlation for $f \times Re_b^{\alpha}$ must be obtained in order to apply the generalization method properly. With this objective, different expressions will be tested:

1. Expression with two parameters,

$$f \times Re_b^{\alpha} = a\, c^{n-1} \tag{13}$$

2. Expression with three parameters,

$$f \times Re_b^{\alpha} = a\, c^{n-1}\, n^d \tag{14}$$

3. Expression with four parameters,

$$f \times Re_b^{\alpha} = a \left(\frac{c\, n^2 + d\, n + e}{(c+d+e)n^2} \right)^n \tag{15}$$

, where a, c, d and e are correlation constants (the letter b has been omitted to avoid confusion). As in previous section, the exponent of the Reynolds number α has been included due to the peculiar nature of the AR-SSHE, where the flow does not exactly behave as in a uniform cross section geometry.

Table 3: Correlation results.

(a) EG1.

	Ec. 13	Ec. 14	Ec. 15
α	0.974	0.974	0.974
a	39.742	41.403	41.729
c	15.536	262.27	212.8
d		-2.1177	-319.16
e			158.93
Error (%)	15.9	11.4	9.6

(b) EG2.

	Ec. 13	Ec. 14	Ec. 15
α	0.951	0.951	0.951
a	33.786	34.070	34.078
c	12.574	80.555	75.852
d		-1.4419	-95.224
e			50.102
Error (%)	12.7	9.0	9.0

The results of the different approaches can be seen in Table 3[1]. The three correlations proposed perform better than the one proposed by Delplace and Leuliet (1995). The lower error corresponds to Eq. 15 followed by Eq. 14, both presenting good agreement with experimental data. Both correlations are plotted in Fig. 10 versus experimental results.

To our understanding, Eq. 14 offers a good approach to experimental results with just three parameters, two of which will appear in the generalized viscosity definition.

In order to define a generalized Reynolds number and viscosity, according to Delplace and Leuliet (1995) $\phi(1) = 1$ in Eq. 16, so

$$Re_g = \frac{Re_b}{\phi(n)} \tag{16}$$

, consequently

$$\phi(n) = c^{n-1}\, n^d \tag{17}$$

$$Re_g = \frac{\rho u_b^{2-n} D^n}{m\, c^{n-1}\, n^d} \tag{18}$$

$$\mu_g = m\, c^{n-1}\, n^d \left(\frac{u_b}{D_h}\right)^{n-1} \tag{19}$$

Pressure drop results are shown in Fig. 11 and Fig. 12 with the generalized Reynolds number defined by Eq. 18. The figure shows as the experimental data for fluids with different pseudoplastic behaviour (different n) can be represented with a single curve in the laminar flow region, while some differences arise in transition flow region.

The proposed generalization method has more parameters than the equation from Delplace and Leuliet (1995), but correlates better with the ex-

[1]The procedure to obtain α is explained in section 3.4.

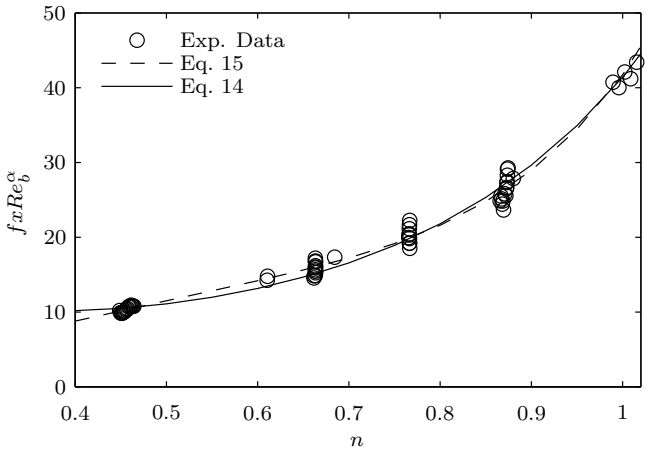

(a) EG1

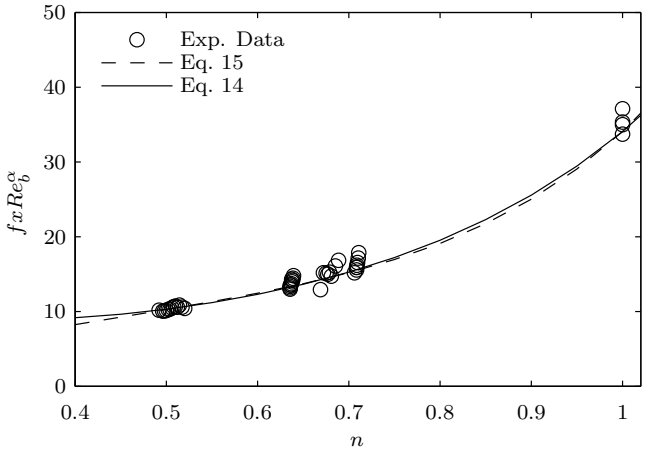

(b) EG2

Figure 10: Comparison between experimental results and experimental correlations.

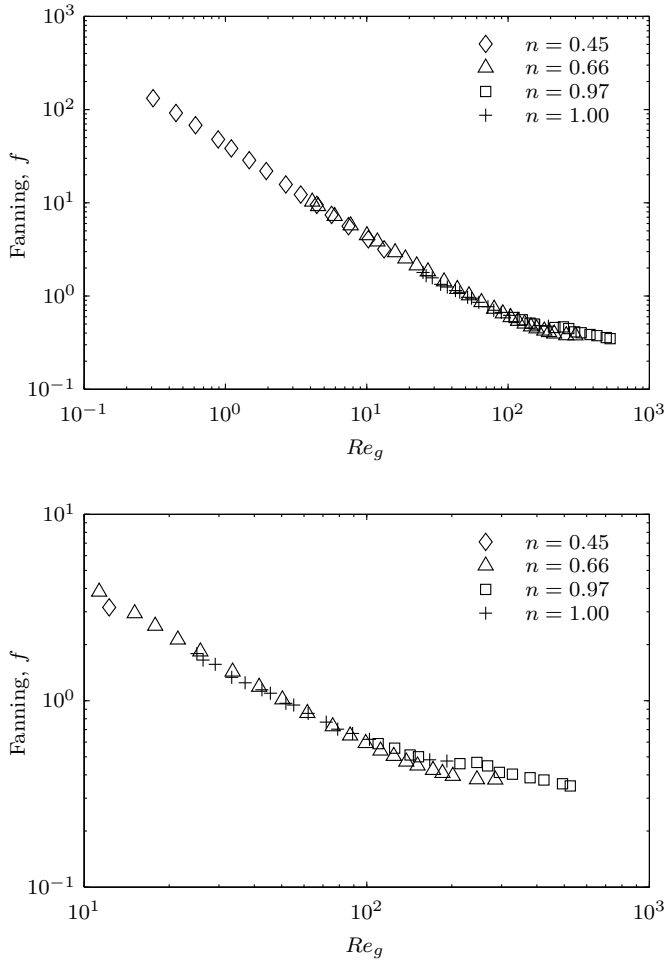

Figure 11: EG1. Generalized Reynolds number Re_g (Eq. 18) versus Fanning friction factor.

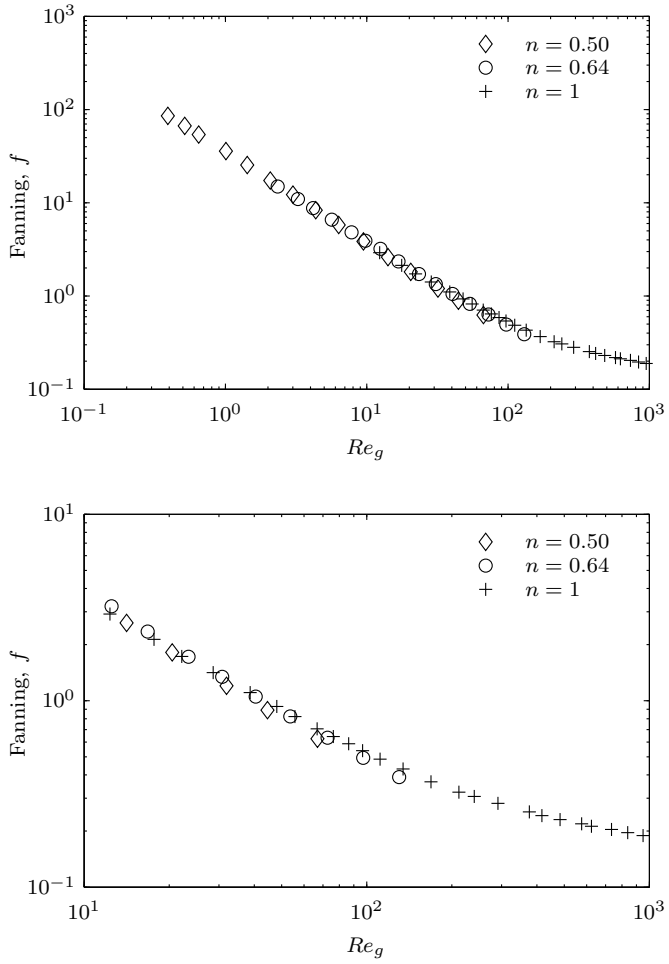

Figure 12: EG2. Generalized Reynolds number Re_g (Eq. 18) versus Fanning friction factor.

perimental data, being still very simple (see Table 2 and Table 3). This generalization method allows to reduce complexity in hydrodynamical problems, where the dependence of n is included in the viscosity definition. The method can be followed in similar heat exchangers devices in order to obtain a valid expression for the generalized viscosity and the generalized Reynolds number.

The expression obtained for the generalized Reynolds number and viscosity (Eq. 18 and Eq. 19) will be valid for this design of heat exchanger, working with any non Newtonian fluid whose behaviour can be modelled with the Power Law model. Obviously, care must be taken that the values of m and n, obtained for the working fluid, are valid in the working range of shear stress.

3.4. Additional comments on the experiments and the correlations obtained

A total of 161 experiments for the EG1 geometry and 101 for EG2 have been carried out. Those experiments belong to laminar, transition and turbulent regions. For all the correlations in this work, only experiments under $Re_g < 40$ have been used to ensure they belong to the laminar region. All the experiments with $Re_g < 40$ are represented in Figures 5, 8 and 10. As, at first, the definition of Re_g is unknown, the first selection has been done by using $Re_{DL,\xi=an} < 40$ and corrected with Re_g at the end if necessary. The number of experiments which satisfy the previous condition are 61 and 47 for EG1 and EG2 geometries respectively. In spite of the restriction imposed ($Re_g < 40$), in Figures 11 and 12 it can be appreciated that the behaviour of the different fluids in the AR-SSHE is represented by a single curve in the whole laminar region ($Re_g < 100$). This means that the generalized Reynolds

number and viscosity definitions are valid in that range.

In order to perform correlations of equations 12, 13, 14 and 15, the exponent of the Reynolds number α has been obtained first. For that, a correlation for the friction factor has been obtained in $f = \Psi(Re_b, n)$ as indicated by each equation. Afterwards, that value of the exponent α has been used to correlate $f \times Re_b^{\alpha}$ as a function of n according to each equation. This procedure allows to minimize the correlating error due to high scaling differences in the Fanning friction factor.

4. Conclusions

In this work, a generalization method in ducts of non uniform cross-section has been presented and experimentally evaluated in two commercial scraped surface heat exchangers.

- Pressure drop of a pseudoplastic non-Newtonian fluid has been experimentally determined in two scraped surface heat exchangers (EG1 and EG2) in static conditions. Experiments have been carried out in a wide range of Reynolds numbers $Re_g = [0.3,\ 600]$ and with Newtonian and non-Newtonian fluids with different degree of pseudoplasticity $n = [0.45,\ 1]$.

- The performance of a generalization method based on the annulus geometry has been tested and found inadequate. Theoretical results for $f \times Re_b^{\alpha}$ in annulus underestimates the experimental data on average in 34% and in 27% in geometries EG1 and EG2 respectively (in laminar region $Re_g < 40$). Furthermore, the representation of the friction factor

versus the generalized Reynolds number based on the annulus geometry is still dependent on the flow behaviour index $f = \Psi(n, Re_{DL,\xi=an})$ in the laminar region. Therefore, this generalization is invalid.

- As suggested by Delplace and Leuliet (1995), an experimental value of ξ in Eq. 8 has been obtained using the experimental data in laminar region ($Re_{DL,an} < 40$). This equation correlates with an error of 17% and 13% in geometries EG1 and EG2 respectively. Furthermore, representations of f versus $Re_{DL,\xi=exp}$ still shows some dependence on n. This solution is very simple, as it only depends on 1 parameter, but the results can be improved.

- A more precise and still simple correlation for the generalization method has been proposed. The proposed correlation estimates $f \times Re_b^{\alpha}$ with an error of 11% and 9% in geometries EG1 and EG2 respectively and the representation of f versus the generalized Reynolds number with this method Re_g shows no appreciable dependence on n.

- The generalized expressions of the Reynolds number and the viscosity obtained in this work are valid for their use in this specific heat exchanger working with any non Newtonian Power Law fluid.

- The generalized method proposed can be applied to similar heat exchanger designs with complex non-uniform cross sections.

5. Acknowledgements

The first author thanks Mr. Martínez and Dr. Solano for their invaluable contribution to the project and their advise. He also thanks the Spanish

Government, Ministry of Education for the FPU scholarship referenced as AP2007-03429 which covered the expenses of a 4-year research at *Universidad Politécnica de Cartagena*.

References

Abdelrahim, K.A., Ramaswamy, H.S., 1995. High temperature/pressure rheology of carboxymethyl cellulose (cmc). Food Research International 28, 285–290.

Abu-Jdayil, B., 2003. Modelling the time-dependent rheological behavior of semisolid foodstuffs. Journal of Food Engineering 57, 97–102.

Benchabane, A., Bekkour, K., 2008. Rheological properties of carboxymethyl cellulose (cmc) solutions. Colloid and Polymer Science 286, 1173–1180.

Cancela, M., Alvarez, E., Maceiras, R., 2005. Effects of temperature and concentration on carboxymethylcellulose with sucrose rheology. Journal of Food Engineering 71, 419–424.

Chhabra, R., Richardson, J., 2008. Non Newtonian flow and applied rheology. Engineering aplications. Butterworth-Heinemann, 225 Wildwood Av., Woburn.

Delplace, F., Leuliet, J., 1995. Generalized reynolds number for the flow of power law fluids in cylindrical ducts of arbitrary cross-section. The Chemical Engineering Journal and the Biochemical Engineering Journal 56, 33 – 37.

Fernandes, C.S., Dias, R.P., Nabrega, J.M., Maia, J.M., 2007. Laminar flow in chevron-type plate heat exchangers: Cfd analysis of tortuosity, shape factor and friction factor. Chemical Engineering and Processing: Process Intensification 46, 825 – 833. Selected Papers from the European Process

Intensification Conference (EPIC), Copenhagen, Denmark, September 19-20, 2007.

Fernandes, C.S., Dias, R.P., Nabrega, J.M., Maia, J.M., 2008. Friction factors of power-law fluids in chevron-type plate heat exchangers. Journal of Food Engineering 89, 441 – 447.

Fyrippi, I., Owen, I., Escudier, M., 2004. Flowmetering of non-newtonian liquids. Flow Measurement and Instrumentation 15, 131–138.

García, A., Vicente, P., Viedma, A., 2005. Experimental study of heat transfer enhancement with wire coil inserts in laminar-transition-turbulent regimes at different prandtl numbers. Int. J. Heat Mass Transfer 48, 4640–4651.

Ghannam, M.T., Esmail, M.N., 1996. Rheological properties of carboxymethyl cellulose. Journal of Applied Polymer Science 64, 289–301.

Giri, A.K., Majumder, S.K., 2014. Pressure drop and its reduction of gas-non-newtonian liquid flow in downflow trickle bed reactor (dtbr). Chemical Engineering Research and Design 92, 34 – 42.

Gratao, A., Jr., V.S., Telis-Romero, J., 2006. Laminar forced convection to a pseudoplastic fluid food in circular and annular ducts. International Communications in Heat and Mass Transfer 33, 451 – 457.

Gratao, A., Jr., V.S., Telis-Romero, J., 2007. Laminar flow of soursop juice through concentric annuli: Friction factors and rheology. Journal of Food Engineering 78, 1343 – 1354.

Hartnett, J., Kostic, M., 1985. Heat transfer to a viscoelastic fluid in laminar flow through a rectangular channel. International Journal of Heat and Mass Transfer 28, 1147–55.

Hong, S., Bergles, A., 1976. Augmentation of laminar flow heat transfer in tubes by means of twisted-tape inserts. ASME J. Heat Transfer 98, 251–256.

Igumentsev, T., Nazmeev, Y., 1978. Intensification of convective heat exchange by spiral swirlers in the flow of anomalously viscous liquids in pipes. J. Eng. Phys. 35, 890–894.

ISO, 1995. Guide to the Expression for Uncertainty Measurement, first ed. International Organization for Standarization, Switzerland.

Kakaç, S., Shah, R., Aung, W., 1987. Handbook of single-phase convective heat transfer. A Wiley Interscience publication, Wiley.

Kozicki, W., Chou, C.H., Tiu, C., 1966. Non-newtonian flow in ducts of arbitrary cross-sectional shape. Chemical Engineering Science 21, 665 – 679.

Manglik, R., Bergles, A., Joshi, S., 1988. Augmentation of heat transfer to laminar flow of non-newtonian fluids in uniformly heated tubes with twisted-tape inserts, in: Elsevier (Ed.), Proceedings of the 1st World Conference on Experimental Heat Transfer, Fluid Mechanics and Thermodynamics, New York.

Marner, W., Bergles, A., 1985. Augmentation of highly viscous laminar

tubeside heat transfer by means of a twisted-tape insert and an internally finned tube. ASME HTD 43, 19–28.

Martínez, D., García, A., Solano, J., Viedma, A., 2014. Heat transfer enhancement of laminar and transitional newtonian and non-newtonian flows in tubes with wire coil inserts. International Journal of Heat and Mass Transfer 76, 540–548.

Metzner, A.B., Reed, J.C., 1955. Flow of non-newtonian fluids - correlation of the laminar, transition, and turbulent-flow regions. Aiche Journal 1(4), 434–440.

Nazmeev, Y., 1979. Intensification of convective heat exchange by ribbon swirlers in the flow of anomalously viscous liquids in pipes. J. Eng. Phys. 37, 910–913.

Oliver, D., Shoji, Y., 1992. Heat transfer enhancement in round tubes using different tube inserts: non-newtonian liquids, trans. IChemE 70, 558–564.

Patil, A., 2000. Laminar flow heat transfer and pressure drop characteristics of power-law fluids inside tubes with varying width twisted tape inserts. J. Heat Transfer 122, 143–149.

Rene, F., Leuliet, J., Lalande, M., 1991. Heat transfer to newtonian and non- newtonian food fluids in plate heat exchangers: experimental and numerical approaches. Trans IChemE 69, 115–126.

Solano, J., García, A., Vicente, P., Viedma, A., 2011. Flow field and heat transfer investigation in tubes of heat exchangers with motionless scrapers. Applied Thermal Engineering 31, 2013–2024.

Webb, R.L., 2005. Principles of Enhanced Heat Transfer. Wiley Interscience.

Yang, X.H., Zhu, W.L., 2007. Viscosity properties of sodium carboxymethyl-cellulose solutions. Cellulose .

List of Figures